

Towards 100% renewable energy systems: The role of hydrogen and batteries

*Original*

Towards 100% renewable energy systems: The role of hydrogen and batteries / Marocco, P., Novo, R., Lanzini, A., Mattiazzo, G., Santarelli, M.. - In: JOURNAL OF ENERGY STORAGE. - ISSN 2352-152X. - 57:(2023), p. 106306. [10.1016/j.est.2022.106306]

*Availability:*

This version is available at: 11583/2973792 since: 2022-12-13T11:08:33Z

*Publisher:*

Elsevier

*Published*

DOI:10.1016/j.est.2022.106306

*Terms of use:*

This article is made available under terms and conditions as specified in the corresponding bibliographic description in the repository

*Publisher copyright*

Elsevier postprint/Author's Accepted Manuscript

© 2023. This manuscript version is made available under the CC-BY-NC-ND 4.0 license  
<http://creativecommons.org/licenses/by-nc-nd/4.0/>. The final authenticated version is available online at:  
<http://dx.doi.org/10.1016/j.est.2022.106306>

(Article begins on next page)

# Towards 100% renewable energy systems: the role of hydrogen and batteries

Paolo Marocco<sup>\*1</sup>, Riccardo Novo<sup>2,3,4</sup>, Andrea Lanzini<sup>1,4</sup>, Giuliana Mattiazzo<sup>2,3,4</sup>,  
Massimo Santarelli<sup>1,5</sup>

<sup>1</sup>Dipartimento Energia "Galileo Ferraris", Politecnico di Torino, 10129, Torino,  
Italy

<sup>2</sup>Dipartimento di Ingegneria Meccanica e Aerospaziale, Politecnico di Torino,  
10129, Torino, Italy

<sup>3</sup>MOREnergy Lab, Politecnico di Torino, 10129, Torino, Italy

<sup>4</sup>Energy Center Lab, Politecnico di Torino, 10129, Torino, Italy

<sup>5</sup>CO<sub>2</sub> Circle Lab, Politecnico di Torino, 10129, Torino, Italy

\*Corresponding author: paolo.marocco@polito.it

## Abstract

New challenges arise for the accurate modelling of energy systems with a high share of renewable energy. In this context, energy storage technologies become key elements to manage fluctuations in renewable energy sources and electricity demand. The aim of this work is to investigate the role of batteries and hydrogen storage in achieving a 100% renewable energy system. First, the impact of time series clustering on the multi-year planning of energy systems that rely heavily on energy storage is assessed. The results show good accuracy, even for a small number of representative days, which is necessary to limit the computational burden of the optimisation problem. Then, different configurations of carbon-free energy systems are considered by varying the energy storage solution: only-battery, only-hydrogen, and hybrid scenarios. An island energy system based on photovoltaics and floating offshore wind turbines is used as a demonstrative case study. It is shown that the cost of the only-battery configuration is 155% higher than the cost of the hydrogen-based scenarios. The reason is that the long-term hydrogen-based storage, despite its low round-trip efficiency, avoids costly oversizing of batteries and wind turbines throughout the analysed period. In the selected

33 case study, hydrogen storage reduces the total rated power of the wind farm by about 5  
34 times compared to the only-battery system. Hydrogen-based solutions are therefore  
35 crucial in 100% renewable energy systems to achieve energy self-sufficiency in a cost-  
36 effective way.

## 37 **Keywords**

38 Renewable energy systems; Renewable energy sources; Hydrogen; Battery;  
39 Energy storage; Energy modelling

## 40 **1 Introduction**

41 In recent years, there has been growing interest in developing sustainable energy  
42 systems based on renewable energy sources (RESs). The deployment of RESs at a large  
43 scale is the first step in the transition to a low-carbon economy. However, the fluctuating  
44 behaviour of variable RESs, e.g., wind and solar, leads to new challenges in terms of  
45 electric grid management and energy storage. The installed capacity of electrical energy  
46 storage (EES) systems is thus expected to increase significantly in the coming years.  
47 Energy storage solutions can be of different types: mechanical, electrochemical,  
48 chemical, electrical and thermal [1,2]. Batteries offer high efficiency and fast response  
49 time [3], making them ideal candidates when small size and short-term energy storage is  
50 needed. Hydrogen is also expected to become essential as a storage solution in RES-  
51 based scenarios due to its long-term storage capability and high energy density [4].  
52 Hydrogen can be generated in a sustainable way through water electrolysis powered by  
53 renewable energy [5]. Once hydrogen is produced, it can be stored and later reconverted  
54 into electricity according to the so-called power-to-power (PtP) route. Moreover, and  
55 differently from a closed battery (pure role of electrical storage), hydrogen can assume  
56 other roles: as feedstock for production of gaseous and liquid synthetic chemicals via  
57 dedicated power-to-X (PtX) routes in a cross-sector perspective [6]. As highlighted by  
58 Lund *et al.* [7], an integrated cross-sector approach can promote a large penetration of  
59 renewable energy sources, by providing additional flexibility in the energy system. In this  
60 context, the potential integration of the electricity, heat, transport and industrial sectors -  
61 as part of a smart energy system - has been shown to be beneficial in achieving 100%  
62 renewable energy supply [8]. Indeed, sector coupling can mitigate the need for grid  
63 expansion and storage capacity [9].

64 In islands, diesel generators (DGs) are still the most widespread choice for  
65 electricity production [10,11]. Local RESs can represent an effective solution to mitigate  
66 DG-related pollution problems and reduce the cost of electricity [12]. However, the  
67 adoption of EES solutions is crucial to improve the RES exploitation and enhance the  
68 reliability of the power supply service. Accurate sizing of the energy storage is thus  
69 necessary when dealing with hybrid renewable energy systems (HRESs) for stand-alone  
70 applications [13]. In this context, in the literature, increasing attention has recently been  
71 paid to the optimal design of stand-alone HRESs to minimise the system cost while  
72 keeping the energy provision reliable and less polluting [14]. As reported in the review by  
73 Liu *et al.* [15], the combination of PV, wind, diesel, and batteries was proven to be feasible,  
74 cost-effective, and with a low environmental impact. Prina *et al.* [16] showed that the cost  
75 of energy supply increases exponentially as the share of variable RESs increases; the  
76 most challenging and expensive phase of the energy transition is from 70% to 100% of  
77 the RES share. High-RES penetration, indeed, entails the oversizing of the HRES  
78 components, with consequent sharp rise in the cost of energy [17]. In this context, the  
79 use of hydrogen was found to be effective in limiting the cost increase when pursuing full-  
80 RES system configurations in off-grid insular communities [18]. The hybridisation of  
81 batteries with hydrogen can represent a cost-effective choice when relying on local RESs  
82 in isolated areas [19]. A 35% cost reduction was reported for the hybrid hydrogen-battery  
83 configuration compared to the only-battery system in a 100% RES-based scenario [20].

84 As shown in the review article by Chang *et al.* [21], there is a wide range of tools  
85 for modelling energy systems: from commercially available software, to open-access  
86 modelling frameworks, and in-house proprietary tools. Current research trends seek to  
87 address cross-sector synergies and improved temporal detail, with an increasing focus  
88 on open-access models. Several modelling methods have been used to investigate the  
89 decarbonisation of islands. HOMER is a well-known commercial software mainly used for  
90 the optimal sizing of RES-based energy systems at the micro-grid level. It can combine  
91 many components and perform optimisation and sensitivity analyses, which simplifies the  
92 evaluation of the most favourable system configuration [22,23]. Metaheuristic-based  
93 models are also widely employed for micro-grid applications to perform the optimal design  
94 of HRESs [24]. When dealing with the energy planning at the whole-island level,  
95 established modelling frameworks include EnergyPLAN, TIMES and OSeMOSYS [25].  
96 They were originally designed for applications at the country level, but have been applied

97 extensively at the island level as well [15]. These tools typically use the linear  
98 programming (LP) or mixed integer linear programming (MILP) techniques to solve the  
99 energy planning problem. TIMES [26] and OSeMOSYS [27] are based on a multi-year  
100 time horizon approach, which allows overcoming intrinsic problems associated with a  
101 single-year formulation. Indeed, the single-year-based framework cannot describe  
102 important phenomena, such as an increase in energy demand over the project lifetime,  
103 changes in long-term behaviour of RESs and changes in the cost of technologies over  
104 time. However, in multi-year capacity expansion models, time series must be  
105 approximated to reduce the computational burden of the simulation. Each year is  
106 generally divided into time slices, which are identified by a season, a day type (i.e., day  
107 of a season) and a daily time bracket (i.e., fraction of the day) [28]. Increasing the number  
108 of time slices improves the accuracy of the time series representation, but at the expense  
109 of a more complex problem. The study of scenarios with high RES penetration, and the  
110 consequent introduction of EES solutions in energy systems, makes the correct  
111 representation of time series even more important [29]. Novo *et al.* [30] addressed this  
112 issue by investigating techniques to reduce the number of time slices and limit the  
113 computational time when dealing with multi-year energy system models. In particular,  
114 they evaluated the advantages of time series clustering and showed good accuracy of  
115 results when only a few representative days (RDs) are used. The benefits of  
116 representative days have also been demonstrated in other works, where a single-year  
117 modelling approach has been adopted [31–33]. Gabrielli *et al.* [31] pointed out that the  
118 interconnection of RDs (based on the chronological order of days over the year) is  
119 necessary to accurately model multi-energy systems with seasonal energy storage [31].  
120 Consistent with this finding, Kotzur *et al.* [32] showed that uncoupled representative  
121 periods are not suitable for modelling energy systems based on high-capacity energy  
122 storage. Hoffmann *et al.* [33] reported that the optimal choice of aggregation methods  
123 depends on the mathematical structure of the energy system optimisation model. They  
124 also showed that the use of representative days is the Pareto-optimal aggregation  
125 approach when storage is considered.

126 This work assesses the impact of time series clustering in the long-term planning  
127 of energy systems, making use of interconnected clustered representative days.  
128 OSeMOSYS, an open-source multi-year modelling framework, was employed in the  
129 present study, further investigating the methodology introduced in [30]. Specifically, a

130 comparative assessment of the traditional and updated OSeMOSYS versions was  
131 conducted to evaluate the effectiveness of the proposed methodology to model the multi-  
132 year evolution of renewable-based energy systems that rely heavily on energy storage.  
133 The island of Pantelleria (in southern Italy) was considered as a demonstrative case study  
134 for this analysis. A relatively simple reference energy system was used to better highlight  
135 the impact of interconnected clustered RDs in modelling long-term energy storage. Then,  
136 different configurations of carbon-free power systems were analysed by varying the EES  
137 solution to shed light on the role of batteries and hydrogen in achieving 100% renewable  
138 energy systems. Specifically, the only-battery, only-hydrogen, and hybrid (i.e., battery  
139 plus hydrogen) configurations were examined.

140 The structure of this work is the following: Section 2 describes the methodology  
141 that has been developed for the energy system modelling. This section also presents the  
142 selected case study and the various scenarios that will be investigated. The main results  
143 are then shown and discussed in Section 3, and finally, the key conclusions are summed  
144 up in Section 4.

## 145 **2 Materials and methods**

146 This section depicts the overall methodology implemented in this paper to explore  
147 the future role of batteries and hydrogen in energy systems with a high share of renewable  
148 energy. First, the modelling framework used is depicted. Then, the model of the insular  
149 energy system is presented along with the main techno-economic assumptions. Finally,  
150 the strategy identified for the development of different energy scenarios is described.

### 151 **2.1 Modelling framework**

152 The energy model has been developed using OSeMOSYS, an LP-/MILP-based,  
153 open-source, multi-year energy modelling framework [27]. In this work, both the  
154 conventional OSeMOSYS version [34] and the enhanced version presented by Novo *et*  
155 *al.* [30] were used. For both versions, an additional set of equations was introduced to  
156 enable a discussion about the storage systems analysed in this article.

157 The structure of OSeMOSYS is based on the following elements: sets, which  
158 determine the model structure; parameters, which are the model inputs; variables, which  
159 are the outputs of the model; and equations, which relate parameters and variables. Each  
160 parameter and variable is a function of one or more sets.

161 The physical model structure is based on the following sets: *regions*, which are  
 162 areas where the balance between supply and demand is guaranteed; *fuels*, which are the  
 163 energy commodities; *technologies*, which are the elements that transform, import or  
 164 export *fuels*; and *storages*, which are used to store *fuels* between time intervals.

165 The objective function (OF) is to minimise the net present cost (NPC) of the energy  
 166 system [35]. As shown in Eq. (1), OF is given by the sum of the discounted costs of all  
 167 *technologies* ( $t$ ) and *storages* ( $s$ ) over all *regions* ( $r$ ) and *years* ( $y$ ). The discounted costs  
 168 can include capital, fixed and variable terms.

169

$$OF = \min \left( \sum_r \sum_y \left( \sum_t TotalDiscountedCostByTechnology_{r,t,y} \right. \right. \\ \left. \left. + \sum_s TotalDiscountedStorageCost_{r,s,y} \right) \right) \quad (1)$$

170

171 where the  $TotalDiscountedCostByTechnology_{r,t,y}$  is the total discounted cost of the  $t$ -  
 172 th *technology* in the  $y$ -th year, and  $TotalDiscountedStorageCost_{r,s,y}$  is the total discounted  
 173 cost of the  $s$ -th *storage* in the  $y$ -th year.

174 The key decision variables are the annual installed capacity of *technologies* and  
 175 *storages* in each year and the activity of *technologies* and *storages* (i.e., a measure of  
 176 their operation) in each time interval.

### 177 2.1.1 TRAD method

178 The time representation in the common version of OSeMOSYS is the same as that  
 179 of typical LP/MILP-based frameworks for long-term optimal expansion planning of energy  
 180 systems [27]. It makes use of five sets: *years* ( $y$ ), *seasons* ( $ls$ ), *daytypes* ( $ld$ ),  
 181 *dailytimebrackets* ( $lh$ ) and *timeslices* ( $l$ ). Each modelled year consists of several *seasons*  
 182 (e.g., spring, summer); *daytypes* (e.g., weekdays, weekends) recur in every *season*; and  
 183 every *daytype* consists of several *dailytimebrackets* (e.g., morning, afternoon). The  
 184 combination of a *season*, a *daytype*, and a *dailytimebracket* represents a *timeslice*. All  
 185 time-related input profiles (e.g., power load profiles, variable RES capacity factors) are  
 186 obtained by averaging original (e.g., hourly) time series. This process - which is performed  
 187 based on how *seasons*, *daytypes* and *dailytimebrackets* recur over the year - is necessary  
 188 to reduce the complexity of the problem and allow the resolution of multi-year optimal

189 planning problems [28]. Nevertheless, such a practice tends to flatten peaks and troughs,  
190 favouring low-cost variable renewables and underestimating the total system cost [36].  
191 Especially, this conventional approach (named TRAD from now on) may lead to a weak  
192 dimensioning of energy storage systems [37].

193 Accurate representation of energy storage becomes increasingly important as the  
194 share of electricity from renewable sources increases. Concerning the energy storage  
195 modelling, OSeMOSYS enables energy to be either stored or discharged during a  
196 *timeslice* as long as the storage level remains within specified minimum and maximum  
197 values. A timeline of *timeslices* is obtained by assigning each *timeslice* to a *season*, a  
198 *daytype* and a *dailytimebracket*, which is needed for a correct modelling of the energy  
199 storage. However, as discussed in [38], it is not necessary to verify that the storage levels  
200 are within their boundaries at each time interval over the year. Indeed, based on the  
201 TRAD time representation, extreme storage level values can only occur during the first  
202 and last week of a specific *season*, and during the first and last occurrences of a particular  
203 *daytype*.

#### 204 **2.1.2 NEW method**

205 In this analysis we considered, and further investigated, the OSeMOSYS update  
206 proposed by Novo *et al.* [30], where interconnected clustered representative days were  
207 implemented to improve the modelling of energy systems with high RES share [39].

208 In contrast to TRAD, where sequential averaging of time series is performed, in  
209 the NEW method representative days are defined using a clustering procedure based on  
210 specific attributes, namely time series profiles of RES supply and electricity demand.

211 As displayed in Figure 1, the first step is to cluster the time series: the aim is to  
212 merge all days of the year into a predefined number of groups (representative days) so  
213 that the group members are as similar as possible. The clustering process was performed  
214 through the k-means algorithm [32]. According to this technique, clusters are created by  
215 minimising the squared error between the empirical mean of a cluster and all candidates  
216 in the cluster. More specifically, it is minimised a distance measure of some attributes  
217 between each group member. The major advantage related to the k-means method is  
218 that the total value of the original time series is preserved for each attribute. In this work,  
219 the following attributes were considered for the clustering: PV capacity factor, wind  
220 capacity factor and electricity demand. At the end of the clustering procedure, each day  
221 of the year is assigned to one of the representative days.

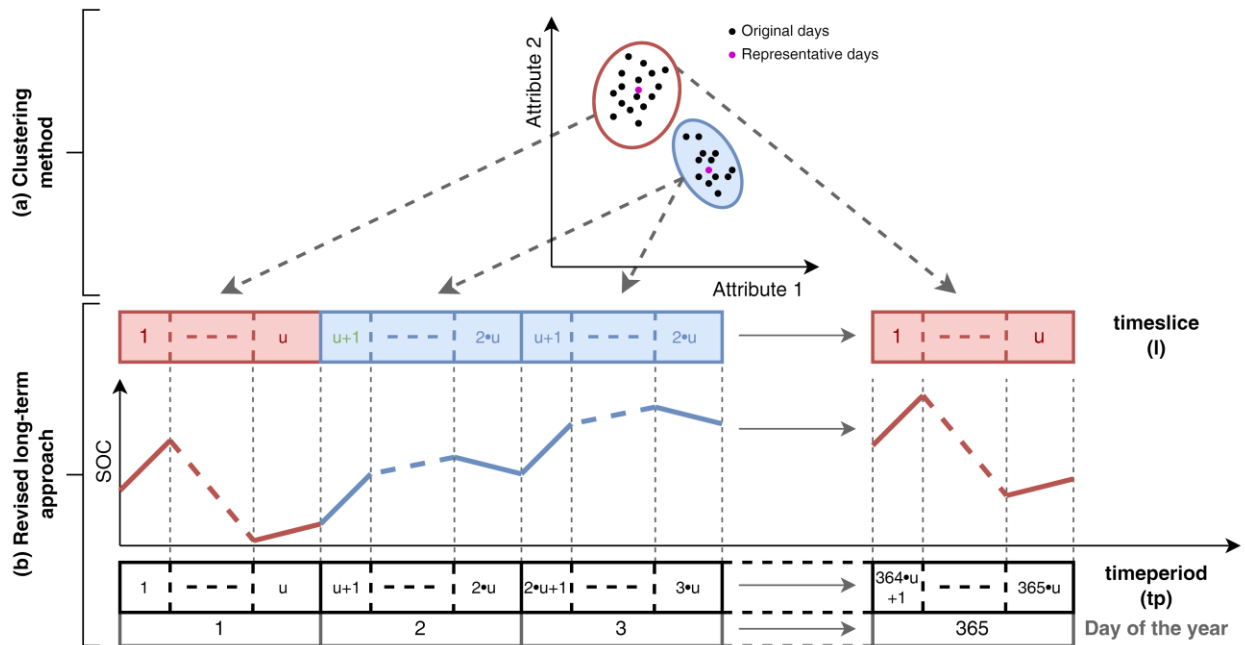
222 Figure 1 also shows that each day consists of a certain number ( $u$ ) of time  
223 intervals. Section 2.2 provides details on the accuracy that has been adopted for the  
224 intraday variability (Table 2). The number of *timeslices* of the model is thus given by  $u$   
225 multiplied by the number of representative days.

226 The TRAD framework was then revised to allow the implementation of clustered  
227 time series while considering the chronological order of the representative days (and thus  
228 *timeslices*) throughout the year. This chronological sequence is necessary for the  
229 modelling of the energy storage.

230 In particular, a new temporal set, called *timeperiod* ( $tp$ ), was introduced to account  
231 for the chronology of *timeslices* over the course of the year. The number of *timeperiods*  
232 is equal to  $u$  (i.e., the time intervals of a day) multiplied by the number of days in a year.  
233 Each *timeperiod* is assigned a *timeslice* on the basis of the RD associated with the day  
234 of that *timeperiod*. The introduction of *timeperiods* eliminates the need for *seasons*,  
235 *daytypes* and *dailytimebrackets*, which are required instead in the TRAD method.

236 As shown in Figure 1, the energy balance of the *storage*, and thus its State-Of-  
237 Charge (SOC) variation, is always the same when a certain *timeslice* occurs in the year.  
238 However, the SOC at the beginning of each *timeperiod*  $tp$  is evaluated based on the SOC  
239 at the beginning of the previous *timeperiod*  $tp-1$  and the SOC variation in the *timeslice*  
240 associated with the *timeperiod*  $tp-1$ . This formulation allows successive time intervals of  
241 the year to be interconnected and was introduced to model the *storages* and describe  
242 their long-term operating cycles when dealing with clustered time series. It should be  
243 noted that, unlike the TRAD method, it is necessary to verify that the storage level (i.e.,  
244 SOC value) remains within the SOC limits for each time interval during the year.

245 A sensitivity analysis on the number of representative days must be performed to  
246 assess a reasonable trade-off between accuracy and computational time.



247

248 *Figure 1 – NEW method: Temporal framework with interconnected clustered*  
 249 *representative days (modified from [30]). For the sake of clarity, a clustering process with two*  
 250 *attributes is shown in the figure. However, in this analysis the clustering was performed*  
 251 *considering three attributes: PV and wind capacity factors, and electricity demand. This figure*  
 252 *also refers to a clustering process with two representative days. SOC is the State-Of-Charge of*  
 253 *the storage.*

254

255 This paper goes beyond the work developed in [30], assessing the suitability of  
 256 NEW for an isolated, 100% renewable-based energy system with a hybrid hydrogen-  
 257 battery storage. Moreover, it aims to evaluate the role of storage systems with different  
 258 durations on a long-term scale. It should be marked that the rated power and rated energy  
 259 of storage systems are sized separately in OSeMOSYS, with different costs associated  
 260 to power-related components (which are modelled as *technologies*) and energy-related  
 261 components (which are modelled as *storages*). While this approach performs well for a  
 262 hydrogen-based PtP solution, it is not suitable for batteries. In fact, many electrochemical  
 263 storage technologies (e.g., Li-ion batteries, NaS batteries) are characterised by a well-  
 264 defined range of energy-to-power ratios. For these EES systems, OSeMOSYS (both  
 265 TRAD and NEW methods) has been updated by introducing lower and upper bounds on  
 266 the ratio between the energy size and the power size. The new parameters and storage  
 267 equations, along with the modified OSeMOSYS code, are included in Section 3 of the  
 268 Supplementary Material.

269 **2.2 Energy model**

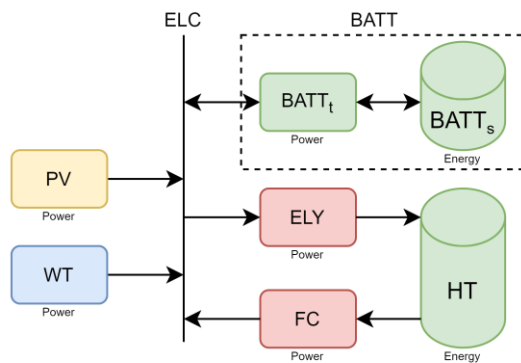
270 The island of Pantelleria was considered as a case study in this analysis. It is  
271 located in the Strait of Sicily, south of Italy, and is not electrically connected to the  
272 mainland. This medium-sized island is a good example of several other insular locations  
273 across the Mediterranean area and thus represents a valuable case study to investigate  
274 solutions for local energy self-sufficiency of remote sites [28].

275 The reference energy system of Pantelleria used in this work is displayed in Figure  
276 2. It includes one *fuel*, five *technologies* and two *storages*. A *storage* set and at least one  
277 *technology* set are needed to model a storage system in OSeMOSYS. *Technologies* are,  
278 indeed, associated to a certain *storage* to enable its charging and discharging.

279 Electricity (ELC) is the *fuel*, which has an associated final demand. The  
280 *technologies* are the following: photovoltaic power plants (PV), floating offshore wind  
281 turbines (WT), electrolyser (ELY), fuel cell (FC), and battery technology (BATT<sub>t</sub>). Two  
282 different *storages* were considered: the hydrogen tank (HT) and the battery storage  
283 (BATT<sub>s</sub>). The ELY and FC are needed, respectively, to charge and discharge the  
284 hydrogen tank. Analogously, the BATT<sub>t</sub> technology was included for the  
285 charging/discharging of the BATT<sub>s</sub> storage.

286 Proton-Exchange Membrane (PEM) electrolysers were considered for hydrogen  
287 production because of their excellent dynamic behaviour, making them suitable for  
288 coupling with variable RESs [40]. The PEM typology was also chosen for the fuel cell  
289 component. As for the BATT component, Li-ion batteries were considered because of  
290 their high roundtrip efficiency, low self-discharge rate and wide cycling modulation range  
291 [18]. Pressurised vessels were assumed for the hydrogen storage tank.

292



293

294

Figure 2 - Reference energy system of the analysed case study.

295  
296 The investigation of renewables-based future energy scenarios requires an  
297 accurate definition of the installable power limits of different technologies. A precise  
298 estimate can be very challenging at a national level; nevertheless, it is more practicable  
299 at the scale of a small island. The PV technical potential for the island of Pantelleria  
300 amounts to 10.8 MW [28]. Such value was obtained as a sum of the 6 MW ground-  
301 mounted PV potential established by the local municipality based on available land, and  
302 the 4.8 MW rooftop PV potential, which would be reached with an average per-capita  
303 installed capacity of around 0.60 kW<sub>PV</sub>/person. Concerning wind power, the installation of  
304 onshore wind turbines of any size is currently forbidden by the Sicilian regional law [41].  
305 Although public authorities are currently engaged in a discussion on the topic, it was  
306 assumed that the current legislative framework is not modified in this analysis. Therefore,  
307 exclusively offshore wind turbines were considered. In addition, because of the very high  
308 depths that characterise the sea in the Strait of Sicily, offshore wind turbines were  
309 supposed to be installed on floating platforms, with a significant increase in the overall  
310 cost of wind power. Specifically, floating wind turbines with a rated power of 2 MW each  
311 were considered in this work.

312 The annual electrical demand in Pantelleria amounted to approximately 27.3 GWh  
313 in 2021, with a power peak of 10.5 MW in the summer period due to tourism. It has been  
314 assumed that the electrical load has an annual increase of 1.5%, mainly because of the  
315 introduction of electric vehicles [28]. A seasonal behaviour is also present in the RES  
316 production profiles: PV (annual production of 1610 kWh/kW) has a peak in the summer  
317 period, whereas floating offshore wind (annual production of 3580 kWh/kW) is  
318 characterised by greater productivity in the winter months, from around January to March.  
319 The strong intra-annual variability of both RES supply and electrical demand profiles  
320 suggests that energy storage systems are necessary to optimise the exploitation of local  
321 RESs and, thus, achieve higher levels of renewable penetration.

322 Table 1 summarises the main techno-economic assumptions to estimate the  
323 CAPEX and replacement costs of the components involved in the Pantelleria energy  
324 system. The values of the operational life are also shown to know when replacements  
325 take place. Cost projections were used for all the components to consider any cost  
326 reductions over the model period, with intermediate values obtained through interpolation.  
327 As suggested by Cole *et al.* [42], the cost of the battery component was divided into

328 power- and energy-related contributions. Cost projections of the PEM electrolyser and  
 329 PEM fuel cell were taken from [43]. It was assumed that the ELY and FC stack  
 330 replacements occur every 10 years [44]. The stack replacement cost was computed as a  
 331 percentage of the CAPEX: 40% for ELY [43] and 50% for FC [45]. OPEX were assessed  
 332 as a fraction of the CAPEX per year [46]. No cost evolution over time was considered for  
 333 the hydrogen tank since the technology of steel pressure vessels is already mature [45].  
 334 Finally, an annual discount rate equal to 4% was adopted in this analysis [46].

335 The charging and discharging efficiency of BATT was set to 95%. A value of 60%  
 336 was assumed for the efficiency of the PEM electrolyser [46], while 51% was used for the  
 337 efficiency of the PEM fuel cell [44]. An energy-to-power ratio range between 0.5 and 2  
 338 was considered for the BATT component (Li-ion typology).

339

340 *Table 1 – Techno-economic assumptions (CAPEX and replacement) of components*  
 341 *involved in the energy system.*

	<b>Capital cost (2021)</b>	<b>Capital cost (2030)</b>	<b>Capital cost (2040)</b>	<b>Operational life (years)</b>	<b>Ref.</b>
<b>PV</b>	1022 k€/MW	523 k€/MW	405 k€/MW	25 y	[47]
<b>WT</b>	3705 k€/MW	2181 k€/MW	2025 k€/MW	25 y	[48]
<b>BATT</b>	500 k€/MW 154 k€/MWh	332 k€/MW 102 k€/MWh	304 k€/MW 89 k€/MWh	10 y	[42,49]
<b>ELY</b>	1300 k€/MW (40% stack)	1000 k€/MW (40% stack)	775 k€/MW (40% stack)	20 y (stack: 10 y)	[43,44]
<b>FC</b>	1520 k€/MW (50% stack)	800 k€/MW (50% stack)	650 k€/MW (50% stack)	20 (stack: 10 y)	[43– 45]
<b>HT</b>	15 k€/MWh	15 k€/MWh	15 k€/MWh	20	[50]

342  
 343 As shown in Table 2, each day was divided into 5 daily time brackets to consider the  
 344 intraday variability of electricity consumption and renewable energy production. This  
 345 detail on the daily variation (which was used for both the TRAD and NEW methods) is  
 346 consistent with assumptions generally made in the literature for long-term energy  
 347 expansion models [37]. The partitioning of days into time intervals is common in long-  
 348 term energy models and is necessary to limit the computational cost and to ensure the  
 349 solvability of the problem.

350  
351

Table 2 – Daily time brackets in every representative day (for both TRAD and NEW methods).

Daily time bracket	Start hour	End hour
1	0	6
2	6	10
3	10	14
4	14	18
5	18	24

352

353 The identification of the cost-optimal configuration of the energy system is allowed  
354 from the first year (2021) onwards. The evolution of the energy system configuration over  
355 the years is related to the increase in the total energy demand and to the cost-learning  
356 curves of the involved components (see Table 1).

### 357 2.3 Scenario setting

358 The validation of the NEW method was done by performing a sensitivity analysis on the  
359 number of representative days, which was increased up to 365. For the validation, the  
360 energy simulation was performed over 1 year in order to solve the full time-scale model  
361 (i.e., 365 representative days), which was used as a reference. The effectiveness of  
362 TRAD as a function of the number of RDs was also analysed for comparison purposes.  
363 In NEW, the required number of RDs was obtained by performing the clustering  
364 procedure described in Section 2.1.2. In TRAD, the RDs were instead derived by  
365 changing the number of *seasons* and considering a single *daytype* for each *season*. It  
366 should be noted that the same number of RDs for TRAD and NEW also implies the same  
367 number of *timeslices*.

368 For each case characterised by a certain number ( $i$ ) of RDs, the relative error in the  
369 objective function (i.e., the net present cost of the system) was evaluated as follows:

370

$$RE_{TRAD/NEW,i} = \frac{OF_{TRAD/NEW,i} - OF_{TRAD,365}}{OF_{TRAD,365}} \quad (2)$$

371

372 where  $RE_{TRAD/NEW,i}$  is the relative error of the TRAD/NEW method with  $i$  RDs, and

373  $OF_{TRAD/NEW,i}$  is the objective function of the TRAD/NEW method with  $i$  RDs.

374 The goal of this sensitivity is to find the minimum number of RDs that can lead to an  
375 accurate representation of the objective function and component sizes. This RD number  
376 was then used to investigate the multi-year evolution of the Pantelleria energy system  
377 (from year 2021 to year 2040). More specifically, different scenarios have been analysed  
378 by varying the configuration of the EES system:

- 379 1. Only-battery scenario: the sizes of the hydrogen-based P2P components (ELY,  
380 FC and HT) are set to zero.
- 381 2. Only-hydrogen scenario: the size of the battery is set to zero.
- 382 3. Hybrid scenario: no size constraints are set on the EES solutions (i.e., hydrogen  
383 and batteries).

### 384 **3 Results and discussion**

385 Simulations were performed on a desktop computer with an Intel® Xeon® CPU  
386 E3-1245 v5 @ 3.50GHz CPU and 32 GB RAM. The IBM ILOG® CPLEX® Optimization  
387 Studio software was employed as solver of the MILP models, imposing a relative MIP gap  
388 tolerance of 0.01%.

389 Representative days were introduced to reduce the complexity of the MILP-based  
390 optimisation framework (Section 3.1). Their influence was assessed using a single-year  
391 model to allow the resolution of the full-scale problem (with all 365 days of the year). The  
392 aim was to identify a sufficiently accurate model to then address the design of multi-year  
393 renewable energy systems (Section 3.2).

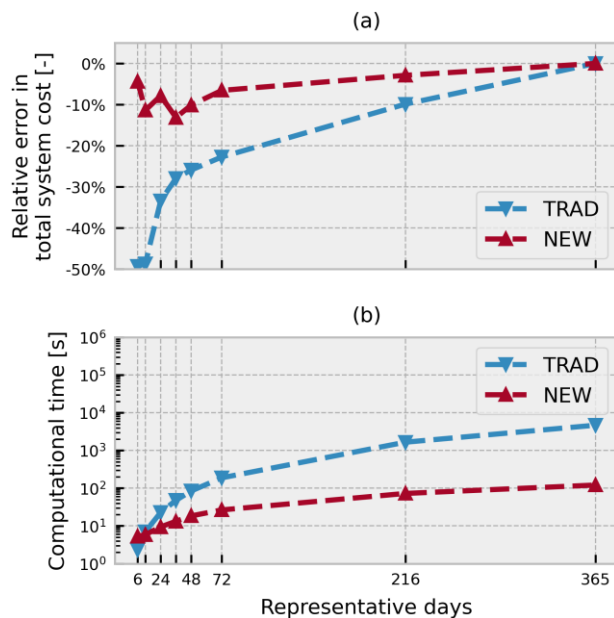
#### 394 **3.1 Impact of representative days**

395 The energy system optimisation was run several times performing a sensitivity  
396 analysis on the number of representative days: from 6 RDs up to the full-scale solution  
397 (i.e., 365 RDs). The goal was to evaluate the minimum number of RDs needed to obtain  
398 an accurate approximation of the full-scale objective function. Moreover, both NEW and  
399 TRAD methods were applied to assess the effectiveness of interconnected clustered RDs  
400 in the modelling of hydrogen-based EES systems. This analysis was performed on a  
401 single year, using the electrical demand profiles and technology costs expected for the  
402 year 2040.

403 The relative error of the objective function with respect to the full-scale model is  
404 depicted in Figure 3a. It can be noted that the relative error of NEW is always lower than  
405 that of TRAD, thus showing that the NEW approach provides better accuracy in

406 estimating the total system cost. When using very few representative days, from 6 to 12,  
 407 the relative error of the traditional method is close to -50%. In contrast, the NEW  
 408 technique can find an optimal system configuration with relative error of around 10%. For  
 409 both methods, the objective function tends to converge by increasing the RD number until  
 410 reaching the same value when 365 representative days are considered.

411 As displayed in Figure 3b, the use of RDs effectively reduces the computational  
 412 burden of the problem. The computational time of the TRAD approach increases from 2.3  
 413 s at 6 RDs to 4679 s at 365 RDs. Moreover, a 23-fold increase can be observed in the  
 414 NEW approach when moving from 6 RDs to the full-scale solution. Although additional  
 415 variables have been added in the NEW approach (related to the modelling of the storage  
 416 component), the TRAD time curve is characterised by a greater slope. This can be due  
 417 to an increase in the number of binary parameters needed to assign a certain *timeslice*  
 418 to a *season* in the TRAD method [30].



419  
 420 *Figure 3 - Relative error in total system cost (a) and computational time (b) for NEW and*  
 421 *TRAD methods as a function of the number of representative days.*

422  
 423 Main sizing outcomes as a function of the number of RDs are displayed in Figure  
 424 4, where the dashed black lines refer to the full-scale solution. The rated power of the PV  
 425 and WT technologies is well approximated over the entire RD interval for both the TRAD  
 426 and NEW methods. The optimal PV size is always equal to 10.8 MW, which corresponds  
 427 to the upper boundary of the PV size decision variable, as pointed out in Section 2.2.

428 Unlike the TRAD approach, the NEW technique can accurately evaluate the battery size,  
429 i.e., rated power and energy, even when very few representative days are used. The  
430 benefits of NEW are also evident in estimating the size of the hydrogen-based  
431 components, i.e., electrolyser, fuel cell and hydrogen tank. The ELY and FC sizes quickly  
432 converge close to the full-scale solution when the NEW approach is used. Compared to  
433 TRAD, NEW also identifies a more accurate value of the HT rated energy in all the RD  
434 configurations. As for the TRAD technique, the HT capacity is almost null in the range  
435 from 6 to 12 RDs. The error on the HT capacity reaches -35% of the full-scale size when  
436 using 24-48 RDs and then gradually improves to the full-scale solution. By contrast,  
437 considering the NEW method, the underestimation of the HT rated energy is always less  
438 than 12% from 12 RDs onwards. The use of interconnected clustered RDs (i.e., the NEW  
439 approach) is thus effective in predicting the long-term storage capacity of the hydrogen  
440 tank, whose optimal rated energy (1365 MWh) is much higher than that of the battery  
441 (1.73 MWh).

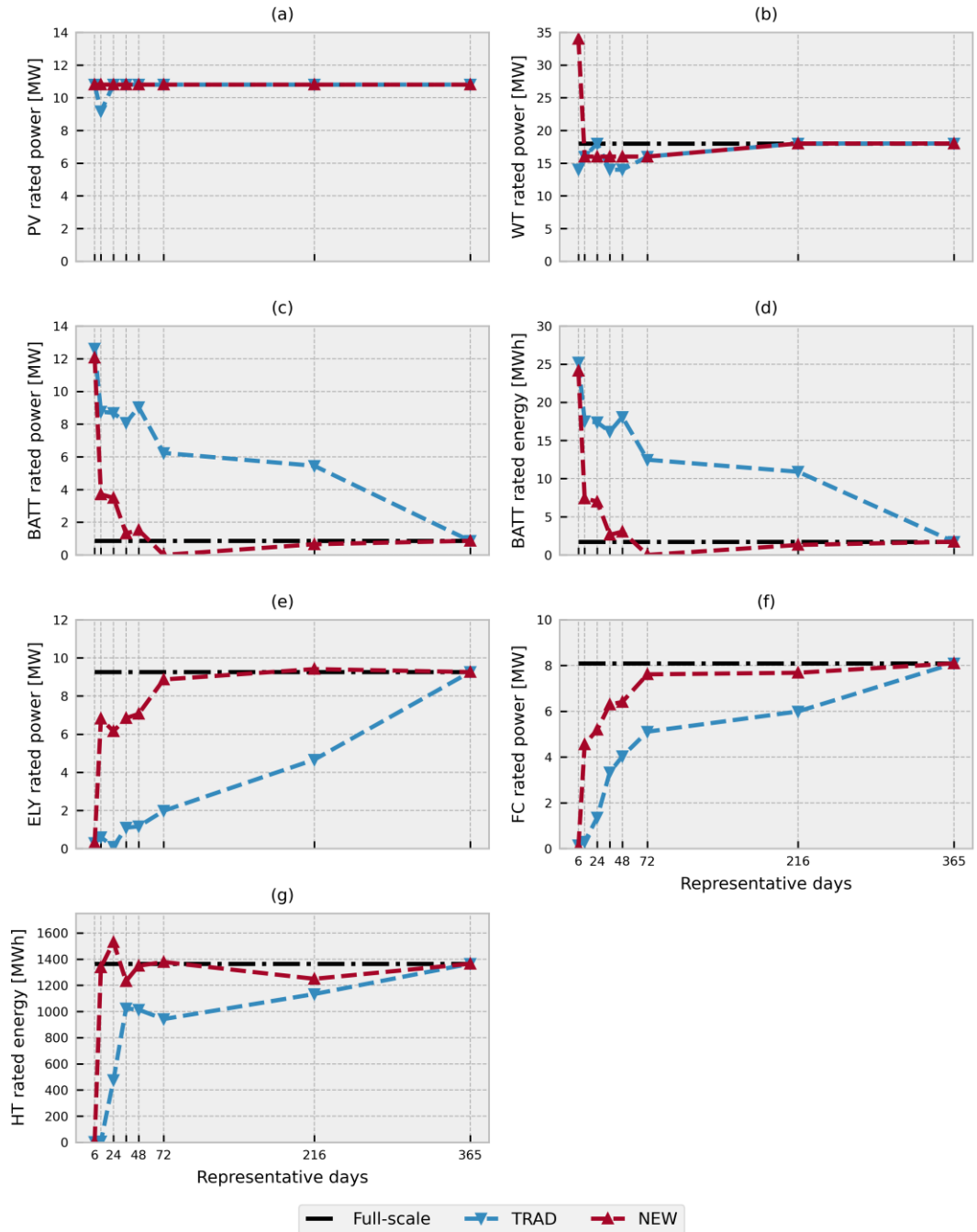
442 Overall, representative days have been demonstrated to reduce the required  
443 simulation time while maintaining a good accuracy in the OF estimation. They were thus  
444 employed for the development of the 20-year energy system model of Pantelleria island,  
445 whose full-scale resolution is unfeasible with the available hardware.

446 It should be noted that the current work is mainly focused on validating the newly  
447 introduced methodology in an energy system characterised by long-term energy storage  
448 and on developing a comparative discussion about the functionality of batteries and  
449 hydrogen in a 100% renewable energy scenario. However, the obtained results show that  
450 this methodology could also be extended to the modelling of more complex energy  
451 systems, thanks to the reduced computational effort ensured by the use of time slices  
452 and the improved reliability of the model.

453

454

455



456

457 *Figure 4 - PV rated power (a), WT rated power (b), BATT rated power (c), BATT rated*  
 458 *energy (d), ELY rated power (e), FC rated power (f) and HT rated energy (g) in 2040 for TRAD*  
 459 *and NEW methods as a function of the number of representative days. The full-scale solution*  
 460 *refers to 365 representative days.*

461

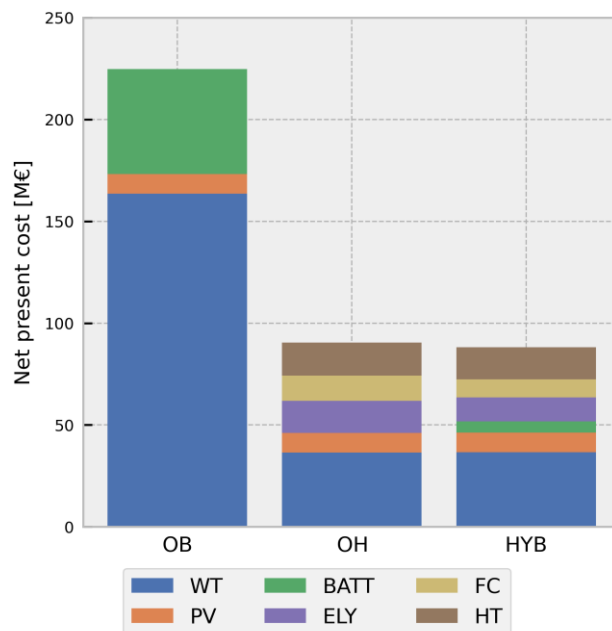
### 462 3.2 Scenarios comparative assessment

463 The multi-year energy model of Pantelleria, from 2021 to 2040, is here presented  
 464 for the NEW approach and considering 48 RDs (240 *timeslices*), which were shown to

465 provide accurate sizing results (see Section 3.1). Three different scenarios have been  
 466 investigated by varying the EES solution: only-battery (OB), only-hydrogen (OH) and  
 467 hybrid (HYB) configurations.

468 The breakdown of the net present cost of the three scenarios is displayed in Figure  
 469 5. The system configuration with hybrid storage is the most cost-effective solution with an  
 470 NPC of 87.9 M€, followed by the only-hydrogen case, whose NPC is slightly higher (90.2  
 471 M€). A 155% NPC increase can be observed when changing from the hybrid to the only-  
 472 battery storage system (224.8 M€). As shown in Figure 5, approximately 70% of the OB  
 473 cost is due to the wind farm subsystem. The battery storage also covers a relevant share  
 474 of the cost (23%). It should be noted that the WT cost decreases significantly, by roughly  
 475 4.5 times, when the hydrogen-based PtP solution is included in the energy system (i.e.,  
 476 OH and HYB scenarios). The implementation of hydrogen storage is thus highly effective  
 477 in limiting the costs when aiming at 100% renewable energy systems. In this case study,  
 478 the PV cost share is the same for the three scenarios since the optimal PV rated power  
 479 is always equal to the maximum installable PV power, i.e., 10.8 MW.

480



481

482  
 483

*Figure 5 - Breakdown of the net present cost (over 20 years project lifetime) in the only-battery (OB), only-hydrogen (OH) and hybrid (HYB) scenarios.*

484

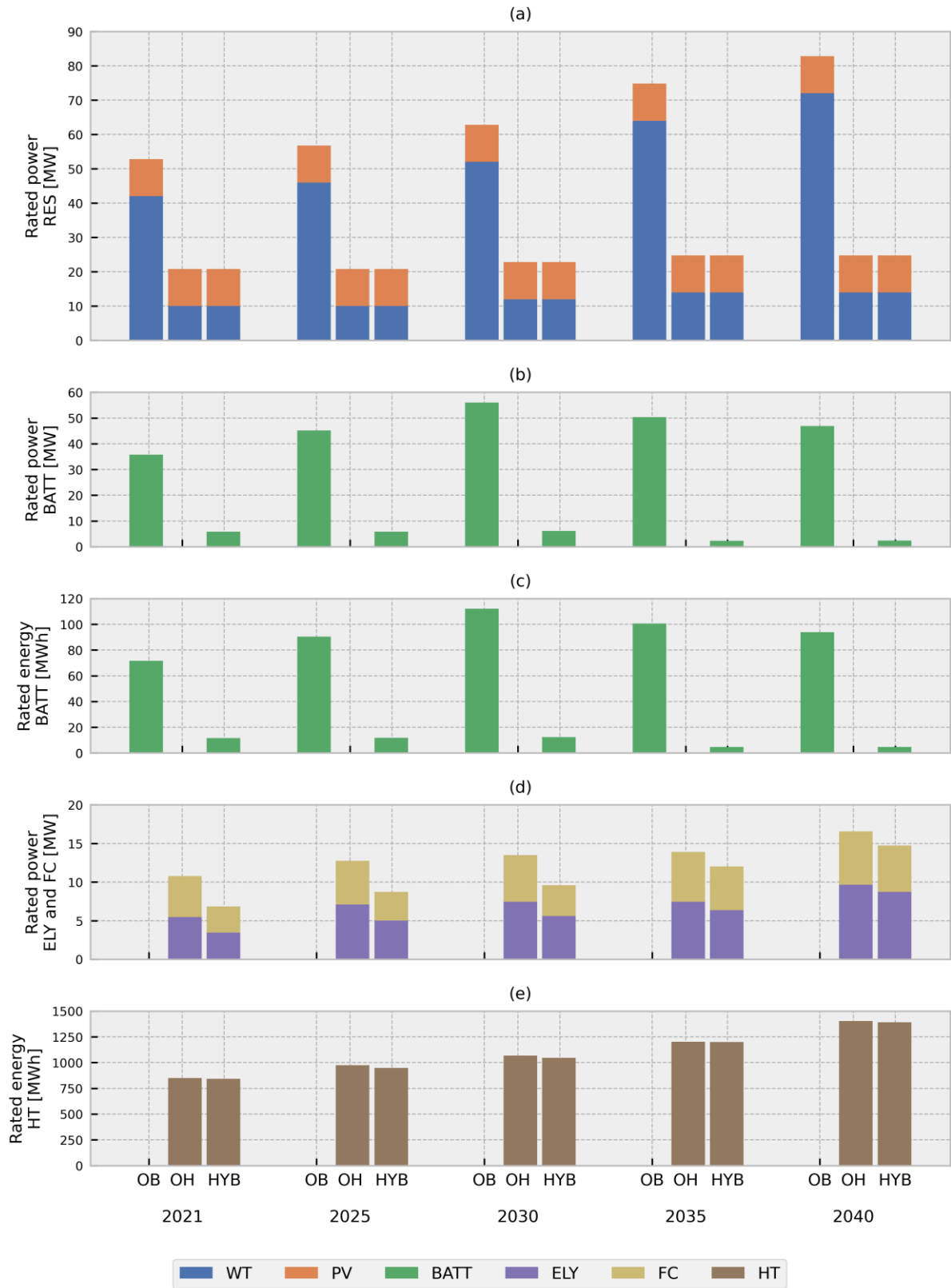
485 The main sizing results over the selected time horizon are reported in Figure 6 for  
486 the OB, OH and HYB scenarios. The corresponding sizing values are specified in the  
487 Appendix, Table A.1.

488 As shown in Figure 6a, in the only-battery scenario, the WT size increases from  
489 42 MW in 2021 to 72 MW in 2040 to cope with the increase in load over years on the  
490 island of Pantelleria. The large WT size of the OB scenario is also accompanied by a  
491 high-capacity battery, whose rated power and energy (in the year 2040) are 46.9 MW and  
492 93.8 MWh, respectively (i.e., energy to power ratio of 2 hours). It can be noted that, in the  
493 OB scenario, the installed battery size has a maximum value in the year 2030 (Figure 6b  
494 and c). From 2030 onwards, the increase in the annual electrical demand is thus mainly  
495 addressed by increasing the WT rated power installed per year, which turns out to be a  
496 cost-optimal planning strategy according to the cost projections reported in Table 1.

497 At the beginning of the project period, the OH and HYB cases require a WT size  
498 of 10 MW, which is about 4 times smaller than that needed in the OB scenario (Figure  
499 6a). However, large-size hydrogen storage is computed for the OH and HYB scenarios,  
500 from 842-851 MWh in 2021 to 1391-1403 MWh in 2040 (Figure 6e). As previously shown  
501 in Figure 5, the H<sub>2</sub>-based power-to-power solution is essential in lowering the cost of the  
502 energy system. In particular, the most cost-effective solution involves the presence of a  
503 hybrid storage system that combines battery and hydrogen technologies. In the HYB  
504 scenario, considering the year 2020, the rated energy of the battery is 73 times smaller  
505 than that of the hydrogen tank (11.6 MWh of BATT compared to 842 MWh of HT). This  
506 size discrepancy further increases over the years: in 2040, indeed, the rated energy of  
507 BATT is 4.7 MWh, while 1391 MWh are foreseen for the HT. The adoption of batteries  
508 has almost no impact on the long-term capacity of the hydrogen tank, which is roughly  
509 the same in the OH and HYB scenarios. However, batteries in the HYB case are useful  
510 to reduce the rated power of the ELY and FC components with respect to the OH case.  
511 As displayed in Figure 6d, in 2021, the ELY size changes from 5.5 MW (OH) to 3.5 MW  
512 (HYB) and the FC size changes from 5.3 MW (OH) to 3.4 MW (HYB). This is because the  
513 short-term BATT storage intervenes in support of the H<sub>2</sub>-based PtP to cover the electrical  
514 demand peaks, thus avoiding oversizing the rated power of the hydrogen equipment.

515 It is also worth noting that, in the OH and HYB scenarios, the increase in the WT  
516 rated power (from 10 MW in 2021 to 14 MW in 2040) is lower compared to the OB  
517 scenario. It is, indeed, more convenient to invest in a greater hydrogen-based storage

518 (and, thus, improve the actual RES exploitation) rather than further increasing the size of  
519 the wind farm. Moreover, it can be observed that the sizing results in 2040 for the multi-  
520 year model differ slightly from the values of the single-year simulation with the same RD  
521 number (see Section 3.1). This is because, in the multi-year approach, the sizing results  
522 at the end of the simulation are influenced by the evolution of the energy system during  
523 previous years.



524

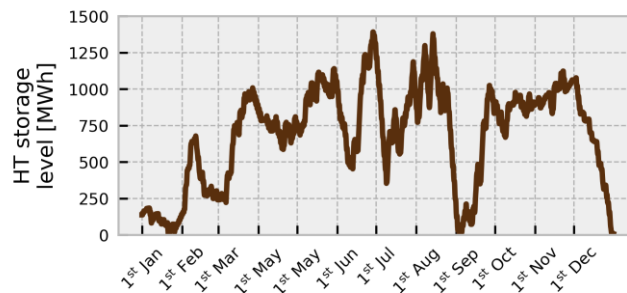
525

526

527

Figure 6 - Main sizing results in the only-battery (OB), only-hydrogen (OH) and hybrid (HYB) scenarios: rated power of PV and WT (a); rated power of BATT (b), rated energy of BATT (c), rated power of ELY and FC (d); and rated energy of HT (e).

528 Figure 7 shows the profile of the energy stored in the hydrogen tank expected for  
529 the year 2040 in the HYB scenario. This trend is typical of a long-term storage system:  
530 the HT is filled during the first part of the year and then emptied during the summer  
531 because of the higher electrical demand. Therefore, the HT function is essential to  
532 maintain a reliable electricity supply service throughout the entire year. On the contrary,  
533 BATT acts as a short-term energy buffer, mainly supporting the hydrogen system during  
534 peak demand.  
535



536  
537 *Figure 7 - Energy stored in the HT storage over the year (2040) in the HYB scenario.*

538  
539 The average round-trip efficiency of the hydrogen-based PtP is 31%, i.e., 60% of  
540 ELY efficiency multiplied by 51% of FC efficiency. This value is three times lower than the  
541 average round-trip efficiency of the BATT-based PtP (90%), given by the product of the  
542 BATT charging (95%) and discharging (95%) efficiencies. However, even if the hydrogen  
543 route is much less efficient than the battery route, hydrogen was found to be crucial to  
544 achieve a cost-optimal 100% renewable energy system. Due to the cost-effective long-  
545 term storage capability of HTs, hydrogen makes it possible to better exploit local  
546 renewable energy sources, thus avoiding a costly oversizing of the RES power plants.  
547 On the island of Pantelleria, in 2021, the WT rated power is 10 MW in the HYB and OH  
548 scenarios and 42 MW in the OB scenario, and this difference in size increases over the  
549 years (14 MW compared to 72 MW in 2040).

550 It is also worth noting that, in the H<sub>2</sub>-based PtP, the rated energy and power are  
551 decoupled and belong to different components, which is a key feature in RES-based  
552 applications when a long-duration EES system is required. In fact, as for the hybrid  
553 scenario, in 2040 the rated power of ELY and FC is 8.7 MW and 6 MW, respectively;  
554 whereas the rated energy of the hydrogen tank is around 1400 MWh, which is needed to

555 cope with the seasonal variation of the electrical demand in Pantelleria. On the contrary,  
556 the rated energy-to-power ratio is constrained in the BATT solution and depends on the  
557 BATT technology adopted. Finally, self-discharge losses, which were not implemented in  
558 this analysis, would shift the results further in favour of hydrogen. They are, in fact, null  
559 for the hydrogen storage but not negligible for the battery solution, especially when  
560 dealing with high-capacity storage systems. However, as shown in the HYB scenario,  
561 batteries are effective and still needed - due to their high efficiency and fast response - to  
562 support the RES-based energy system in daily operation.

## 563 **4 Conclusions**

564 In this work, time series clustering was used to improve the modelling of energy systems  
565 with a high share of renewable energy. Different EES configurations (i.e., only-battery,  
566 only-hydrogen, and hybrid) were investigated to disclose the role of batteries and  
567 hydrogen in 100% renewable-based systems. The main conclusions are summarised  
568 below:

- 569 • The use of interconnected clustered representative days (NEW method) was  
570 shown to be effective to address the modelling of energy systems with long-term  
571 energy storage. Few representative days, from around 48, are needed to obtain  
572 an accurate representation of the objective function (NPC) and the component  
573 sizes. Due to the reduced computational effort, this method can be extended to  
574 the modelling of more complex energy systems.
- 575 • Hydrogen storage plays a key role in achieving cost-effective system  
576 configurations that rely entirely on local RESs. In the case study of Pantelleria, the  
577 NPC of the only-battery energy system is 155% higher than that of the hybrid  
578 (hydrogen + battery) alternative.
- 579 • In the HYB configuration, batteries assume anyway a useful role as short-term  
580 energy buffer, supporting the energy system in daily operation and reducing the  
581 installed rated power of the ELY and FC components.
- 582 • Although the hydrogen-based pathway is less efficient (about three times lower)  
583 than the battery-based pathway, the advantage of hydrogen lies in the low-cost  
584 high-capacity hydrogen tanks, which become crucial in RES-based energy  
585 systems to address the seasonal behaviour of renewable production and electrical  
586 demand. Long-term storage of hydrogen enhances the exploitation of renewable

587 energy, avoiding costly oversizing of renewable generators. As an example, in  
588 2040 the WT rated power in the hydrogen-based scenarios (i.e., OH and HYB) is  
589 around 5 times lower than that needed in the OB scenario.

590 Based on the methodology proposed in this work, future steps will address the  
591 development of a spatially resolved model of the Pantelleria energy system, considering  
592 a multi-nodal approach for a more accurate assessment of RES production across the  
593 island. The impact of intraday variability on sizing results deserves also to be investigated  
594 in future works.

## 595 **Abbreviations and acronyms**

BATT	Battery
CAPEX	Capital Expenditures
DG	Diesel Generator
EES	Electrical Energy Storage
ELY	Electrolyser
FC	Fuel Cell
HRES	Hybrid Renewable Energy System
HT	Hydrogen Tank
HYB	Hybrid
LP	Linear Programming
MILP	Mixed Integer Linear Programming
NPC	Net Present Cost
OB	Only-Battery
OF	Objective Function
OH	Only-Hydrogen
OPEX	Operating Expenditures
PEM	Proton-Exchange Membrane
PtP	Power-to-Power

PtX	Power-to-X
PV	Photovoltaic
RD	Representative Day
RES	Renewable Energy Source
TRAD	Traditional
WT	Wind Turbine

596

## 597 Appendix

598 Main sizing results of the 3 scenarios (OB, OH and HYB) are listed in Table A.1  
 599 for the years 2021, 2030 and 2040.

600

601 *Table A.1 - Main sizing results in the only-battery (OB), only-hydrogen (OH) and hybrid*  
 602 *(HYB) scenarios in 2021, 2030 and 2040 years.*

Scenarios		WT	PV	BATT	BATT	ELY	FC	HT
		[MW]	[MW]	[MW]	[MWh]	[MW]	[MW]	[MWh]
2021	OB	42	10.8	35.8	71.6	-	-	-
	OH	10	10.8	-	-	5.5	5.3	850.9
	HYB	10	10.8	5.8	11.6	3.5	3.4	842
2030	OB	52	10.8	56	112.1	-	-	-
	OH	12	10.8	-	-	7.4	6	1067.7
	HYB	12	10.8	6.1	12.3	5.6	4	1047.4
2040	OB	72	10.8	46.9	93.8	-	-	-
	OH	14	10.8	-	-	9.7	6.9	1403
	HYB	14	10.8	2.4	4.7	8.7	6	1391.3

603

604

## 605 References

606 [1] International Electrotechnical Commission, Electrical Energy Storage - white paper,  
 607 2019. <https://www.iec.ch/basecamp/electrical-energy-storage>.

- 608 [2] X. Luo, J. Wang, M. Dooner, J. Clarke, Overview of current development in  
609 electrical energy storage technologies and the application potential in power  
610 system operation, *Appl. Energy.* 137 (2015) 511–536.  
611 <https://doi.org/10.1016/j.apenergy.2014.09.081>.
- 612 [3] H.C. Hesse, M. Schimpe, D. Kucevic, A. Jossen, Lithium-ion battery storage for the  
613 grid - A review of stationary battery storage system design tailored for applications  
614 in modern power grids, 2017. <https://doi.org/10.3390/en10122107>.
- 615 [4] S. Dutta, A review on production , storage of hydrogen and its utilization as an  
616 energy resource, *J. Ind. Eng. Chem.* 20 (2014) 1148–1156.  
617 <https://doi.org/10.1016/j.jiec.2013.07.037>.
- 618 [5] Z. Abdin, A. Zafaranloo, A. Rafiee, W. Mérida, W. Lipiński, K.R. Khalilpour,  
619 Hydrogen as an energy vector, *Renew. Sustain. Energy Rev.* 120 (2020).  
620 <https://doi.org/10.1016/j.rser.2019.109620>.
- 621 [6] G. Buffo, P. Marocco, D. Ferrero, A. Lanzini, M. Santarelli, Power-to-X and power-  
622 to-power routes, in: *Sol. Hydrog. Prod.*, 2019: pp. 529–557.  
623 <https://doi.org/10.1016/B978-0-12-814853-2.00015-1>.
- 624 [7] H. Lund, P.A. Østergaard, D. Connolly, B.V. Mathiesen, Smart energy and smart  
625 energy systems, *Energy.* 137 (2017) 556–565.  
626 <https://doi.org/10.1016/j.energy.2017.05.123>.
- 627 [8] H. Lund, J.Z. Thellufsen, P. Sorknæs, B.V. Mathiesen, M. Chang, P.T. Madsen,  
628 M.S. Kany, I.R. Skov, Smart energy Denmark. A consistent and detailed strategy  
629 for a fully decarbonized society, *Renew. Sustain. Energy Rev.* 168 (2022).  
630 <https://doi.org/10.1016/j.rser.2022.112777>.
- 631 [9] H. Lund, P.A. Østergaard, D. Connolly, I. Ridjan, B.V. Mathiesen, F. Hvelplund, J.Z.  
632 Thellufsen, P. Sorknses, Energy storage and smart energy systems, *Int. J. Sustain.*  
633 *Energy Plan. Manag.* 11 (2016) 3–14. <https://doi.org/10.5278/ijsepm.2016.11.2>.
- 634 [10] D. Bionaz, P. Marocco, D. Ferrero, K. Sundseth, M. Santarelli, Life cycle  
635 environmental analysis of a hydrogen-based energy storage system for remote  
636 applications, *Energy Reports.* 8 (2022) 5080–5092.  
637 <https://doi.org/10.1016/j.egy.2022.03.181>.
- 638 [11] D. Haase, A. Maier, Islands of the European Union: State of play and future  
639 challenges, 2021.  
640 [26](https://www.europarl.europa.eu/RegData/etudes/STUD/2021/652239/IPOL_STU(</a></p></div><div data-bbox=)

- 641 2021)652239\_EN.pdf.
- 642 [12] X. Qi, J. Wang, G. Królczyk, P. Gardoni, Z. Li, Sustainability analysis of a hybrid  
643 renewable power system with battery storage for islands application, *J. Energy*  
644 *Storage*. 50 (2022) 104682.  
645 <https://doi.org/https://doi.org/10.1016/j.est.2022.104682>.
- 646 [13] S. Hajiaghasi, A. Salemnia, M. Hamzeh, Hybrid energy storage system for  
647 microgrids applications: A review, *J. Energy Storage*. 21 (2019) 543–570.  
648 <https://doi.org/https://doi.org/10.1016/j.est.2018.12.017>.
- 649 [14] R. Siddaiah, R.P. Saini, A review on planning, configurations, modeling and  
650 optimization techniques of hybrid renewable energy systems for off grid  
651 applications, *Renew. Sustain. Energy Rev.* 58 (2016) 376–396.  
652 <https://doi.org/10.1016/j.rser.2015.12.281>.
- 653 [15] Y. Liu, S. Yu, Y. Zhu, D. Wang, J. Liu, Modeling, planning, application and  
654 management of energy systems for isolated areas: A review, *Renew. Sustain.*  
655 *Energy Rev.* 82 (2018) 460–470. <https://doi.org/10.1016/j.rser.2017.09.063>.
- 656 [16] M.G. Prina, V. Casalicchio, C. Kaldemeyer, G. Manzolini, D. Moser, A. Wanitschke,  
657 W. Sparber, Multi-objective investment optimization for energy system models in  
658 high temporal and spatial resolution, *Appl. Energy*. 264 (2020) 114728.  
659 <https://doi.org/10.1016/j.apenergy.2020.114728>.
- 660 [17] O.D.T. Odou, R. Bhandari, R. Adamou, Hybrid off-grid renewable power system for  
661 sustainable rural electrification in Benin, *Renew. Energy*. 145 (2020) 1266–1279.  
662 <https://doi.org/10.1016/j.renene.2019.06.032>.
- 663 [18] P. Marocco, D. Ferrero, A. Lanzini, M. Santarelli, Optimal design of stand-alone  
664 solutions based on RES + hydrogen storage feeding off-grid communities, *Energy*  
665 *Convers. Manag.* 238 (2021) 114147.  
666 <https://doi.org/10.1016/j.enconman.2021.114147>.
- 667 [19] H. Mun, B. Moon, S. Park, Y. Yoon, A study on the economic feasibility of stand-  
668 alone microgrid for carbon-free island in Korea, *Energies*. 14 (2021).  
669 <https://doi.org/10.3390/en14071913>.
- 670 [20] P. Marocco, D. Ferrero, A. Lanzini, M. Santarelli, The role of hydrogen in the optimal  
671 design of off-grid hybrid renewable energy systems, *J. Energy Storage*. 46 (2022)  
672 103893. <https://doi.org/10.1016/j.est.2021.103893>.
- 673 [21] M. Chang, J.Z. Thellufsen, B. Zakeri, B. Pickering, S. Pfenninger, H. Lund, P.A.

- 674 Østergaard, Trends in tools and approaches for modelling the energy transition,  
675 Appl. Energy. 290 (2021). <https://doi.org/10.1016/j.apenergy.2021.116731>.
- 676 [22] C. Mokhtara, B. Negrou, A. Bouferrouk, Y. Yao, N. Settou, M. Ramadan, Integrated  
677 supply–demand energy management for optimal design of off-grid hybrid  
678 renewable energy systems for residential electrification in arid climates, Energy  
679 Convers. Manag. 221 (2020) 113192.  
680 <https://doi.org/10.1016/j.enconman.2020.113192>.
- 681 [23] S. Sinha, S.S. Chandel, Review of software tools for hybrid renewable energy  
682 systems, Renew. Sustain. Energy Rev. 32 (2014) 192–205.  
683 <https://doi.org/10.1016/j.rser.2014.01.035>.
- 684 [24] S. Mohseni, A.C. Brent, D. Burmester, A comparison of metaheuristics for the  
685 optimal capacity planning of an isolated, battery-less, hydrogen-based micro-grid,  
686 Appl. Energy. 259 (2020) 114224. <https://doi.org/10.1016/j.apenergy.2019.114224>.
- 687 [25] M.G. Prina, D. Groppi, B. Nastasi, D.A. Garcia, Bottom-up energy system models  
688 applied to sustainable islands, Renew. Sustain. Energy Rev. 152 (2021) 111625.  
689 <https://doi.org/10.1016/j.rser.2021.111625>.
- 690 [26] R. Loulou, G. Goldstein, A. Kanudia, U. Remme, Documentation for the TIMES  
691 Model Part I: TIMES Concepts and Theory, 2016. [http://www.iea-](http://www.iea-etsap.org/web/Documentation.asp)  
692 [etsap.org/web/Documentation.asp](http://www.iea-etsap.org/web/Documentation.asp) (accessed October 23, 2020).
- 693 [27] M. Howells, H. Rogner, N. Strachan, C. Heaps, H. Huntington, S. Kypreos, A.  
694 Hughes, S. Silveira, J. DeCarolis, M. Bazillian, A. Roehrl, OSeMOSYS: The Open  
695 Source Energy Modeling System. An introduction to its ethos, structure and  
696 development, Energy Policy. 39 (2011) 5850–5870.  
697 <https://doi.org/10.1016/j.enpol.2011.06.033>.
- 698 [28] R. Novo, F.D. Minuto, G. Bracco, G. Mattiazzo, R. Borchiellini, A. Lanzini,  
699 Supporting Decarbonization Strategies of Local Energy Systems by De-Risking  
700 Investments in Renewables: A Case Study on Pantelleria Island, Energies. 15  
701 (2022). <https://doi.org/10.3390/en15031103>.
- 702 [29] L. Kotzur, P. Markewitz, M. Robinius, D. Stolten, Time series aggregation for energy  
703 system design: Modeling seasonal storage, Appl. Energy. 213 (2018) 123–135.  
704 <https://doi.org/10.1016/j.apenergy.2018.01.023>.
- 705 [30] R. Novo, P. Marocco, G. Giorgi, A. Lanzini, M. Santarelli, G. Mattiazzo, Planning  
706 the decarbonisation of energy systems: the importance of applying time series

- 707 clustering to long-term models, *Energy Convers. Manag.* X. 15 (2022) 100274.  
708 <https://doi.org/https://doi.org/10.1016/j.ecmx.2022.100274>.
- 709 [31] P. Gabrielli, M. Gazzani, E. Martelli, M. Mazzotti, Optimal design of multi-energy  
710 systems with seasonal storage, *Appl. Energy.* 219 (2018) 408–424.  
711 <https://doi.org/10.1016/j.apenergy.2017.07.142>.
- 712 [32] L. Kotzur, P. Markewitz, M. Robinius, D. Stolten, Impact of different time series  
713 aggregation methods on optimal energy system design, *Renew. Energy.* 117  
714 (2018) 474–487. <https://doi.org/10.1016/j.renene.2017.10.017>.
- 715 [33] M. Hoffmann, J. Priesmann, L. Nolting, A. Praktiknjo, L. Kotzur, D. Stolten, Typical  
716 periods or typical time steps? A multi-model analysis to determine the optimal  
717 temporal aggregation for energy system models, *Appl. Energy.* 304 (2021) 117825.  
718 <https://doi.org/https://doi.org/10.1016/j.apenergy.2021.117825>.
- 719 [34] OSeMOSYS Community, GitHub OSeMOSYS Pyomo, (2022).  
720 [https://github.com/OSeMOSYS/OSeMOSYS\\_Pyomo](https://github.com/OSeMOSYS/OSeMOSYS_Pyomo) (accessed November 26,  
721 2022).
- 722 [35] KTH Royal Institute of Technology - School of Industrial Engineering and  
723 Management division of Energy Systems Analysis, KTH Royal Institute of  
724 Technology, OSeMOSYS Documentation, 2019.
- 725 [36] K. Poncelet, E. Delarue, D. Six, J. Duerinck, W. D’haeseleer, Impact of the level of  
726 temporal and operational detail in energy-system planning models, *Appl. Energy.*  
727 162 (2016) 631–643. <https://doi.org/10.1016/j.apenergy.2015.10.100>.
- 728 [37] O. Balyk, K.S. Andersen, S. Dockweiler, M. Gargiulo, K. Karlsson, R. Næraa, S.  
729 Petrović, J. Tattini, L.B. Termansen, G. Venturini, TIMES-DK: Technology-rich  
730 multi-sectoral optimisation model of the Danish energy system, *Energy Strateg.*  
731 *Rev.* 23 (2019) 13–22. <https://doi.org/10.1016/j.esr.2018.11.003>.
- 732 [38] M. Welsch, Enhancing the Treatment of Systems Integration in Long-term Energy  
733 Models. Doctoral Thesis., 2013.
- 734 [39] GitHub - revised OSeMOSYS-Pyomo with new timeframe., (2022).  
735 [https://github.com/riccardonovo/OSeMOSYS\\_Pyomo/tree/OSeMOSYS\\_EC\\_2022](https://github.com/riccardonovo/OSeMOSYS_Pyomo/tree/OSeMOSYS_EC_2022)  
736 0118 (accessed November 26, 2022).
- 737 [40] G. Correa, P. Marocco, P. Muñoz, T. Falagüerra, D. Ferrero, M. Santarelli,  
738 Pressurized PEM water electrolysis: Dynamic modelling focusing on the cathode  
739 side, *Int. J. Hydrogen Energy.* 47 (2022) 4315–4327.

- 740 <https://doi.org/10.1016/j.ijhydene.2021.11.097>.
- 741 [41] Clean Energy for EU Islands, Energy Center Lab, Comune di Pantelleria, Parco  
742 Nazionale Isola di Pantelleria, S.MED.E. Pantelleria S.p.A., SOFIP S.p.A., APS  
743 Resilea, Cantina Basile, Agenda per la transizione energetica. Isola di Pantelleria,  
744 2020. <https://clean-energy-islands.ec.europa.eu/countries/italy/pantelleria>.
- 745 [42] W. Cole, A.W. Frazier, C. Augustine, Cost Projections for Utility-Scale Battery  
746 Storage: 2021 Update, 2021. <https://www.nrel.gov/docs/fy21osti/79236.pdf>.
- 747 [43] D. Thomas, D. Mertens, M. Meeus, W. Van der Laak, I. Francois, Power-to-gas  
748 Roadmap for Flanders, Brussels, 2016.  
749 [https://www.waterstofnet.eu/\\_asset/\\_public/powertogas/P2G-Roadmap-for-](https://www.waterstofnet.eu/_asset/_public/powertogas/P2G-Roadmap-for-Flanders.pdf)  
750 [Flanders.pdf](https://www.waterstofnet.eu/_asset/_public/powertogas/P2G-Roadmap-for-Flanders.pdf).
- 751 [44] D.G. Caglayan, H.U. Heinrichs, M. Robinius, D. Stolten, Robust design of a future  
752 100% renewable european energy supply system with hydrogen infrastructure, Int.  
753 J. Hydrogen Energy. 46 (2021) 29376–29390.  
754 <https://doi.org/10.1016/j.ijhydene.2020.12.197>.
- 755 [45] Tractebel, Inicio, Study on early business cases for H2 in energy storage and  
756 more broadly power to H2 applications, 2017.  
757 [https://www.fch.europa.eu/sites/default/files/P2H\\_Full\\_Study\\_FCHJU.pdf](https://www.fch.europa.eu/sites/default/files/P2H_Full_Study_FCHJU.pdf).
- 758 [46] H. Böhm, A. Zauner, D.C. Rosenfeld, R. Tichler, Projecting cost development for  
759 future large-scale power-to-gas implementations by scaling effects, Appl. Energy.  
760 264 (2020). <https://doi.org/10.1016/j.apenergy.2020.114780>.
- 761 [47] International Renewable Energy Agency (IRENA), Future of solar photovoltaic.  
762 Deployment, investment, technology, grid integration and socio-economic aspects,  
763 2019. <https://www.irena.org/publications/2019/Nov/Future-of-Solar-Photovoltaic>.
- 764 [48] International Renewable Energy Agency (IRENA), Future of wind. Deployment,  
765 investment, technology, grid integration and socio-economic aspects, 2019.  
766 <https://www.irena.org/publications/2019/Oct/Future-of-wind>.
- 767 [49] E. Crespi, P. Colbertaldo, G. Guandalini, S. Campanari, Design of hybrid power-to-  
768 power systems for continuous clean PV-based energy supply, Int. J. Hydrogen  
769 Energy. 46 (2021) 13691–13708.  
770 <https://doi.org/https://doi.org/10.1016/j.ijhydene.2020.09.152>.
- 771 [50] M. Reuß, T. Grube, M. Robinius, P. Preuster, P. Wasserscheid, D. Stolten,  
772 Seasonal storage and alternative carriers: A flexible hydrogen supply chain model,

773 Appl. Energy. 200 (2017) 290–302.  
774 <https://doi.org/10.1016/j.apenergy.2017.05.050>.  
775